Proceedings of the 2002 IEEE/RSJ
Intl. Conference on Intelligent Robots and Systems
EPFL, Lausanne, Switzerland • October 2002

Control of Multi-DOF Ultrasonic Motor using Neural Network based Inverse Model

Kenjiro Takemura, Takashi Maeno

Department of Mechanical Engineering, Keio University, kenjiro@mmm-keio.net, maeno@mech.keio.ac.jp

Abstract

A multi-DOF ultrasonic motor developed by the authors is capable of generating multi-DOF rotation of a spherical rotor using three orthogonal natural vibrations of a bar-shaped stator. The ultrasonic motor is suitable for making small, light weight and simple multi-DOF motion unit. In the present paper, a control methodology for the multi-DOF ultrasonic motor is proposed and a motion control test using the method is conducted. First, an inverse model of the multi-DOF ultrasonic motor is developed using our prior knowledge in ultrasonic motors and neural network technique in order to deal with the redundancy and non-linearity of driving characteristics. Second, a novel control method using the inverse model is proposed. Then, motion control tests are conducted to confirm the ability of the proposed control method. The results confirm that the rotor can be rotated around arbitrary rotational axis using the inverse model, and that the proposed control method does work successfully.

1 Introduction

Multi-DOF systems like humanoid robots have high ability to be used for various purposes because they have a great number of DOF. Hence, there are lots of researches on multi-DOF systems in recent years including structure designs, controls and applications of multi-DOF systems. However, such researches potentially have problems on the number of actuators. Namely, they need a large number of actuators to generate effective dexterous motions. The problem always causes the entire system to be heavy, large and complicated. So, researches on multi-DOF actuators have also been conducted in the past decades. For examples of multi-DOF electromagnetic actuators, Roth *et al.* proposed a three DOF variable-reluctance spherical wrist motor [1]. The motor provides three DOF rotation of a spherical rotor using electromagnetic force. Yano *et al.* developed a spherical stepping motor and a synchronous motor with three DOF [2][3]. Sokolov *et al.* developed a spherical direct drive actuator [4]. Ebara *et al.* presented a PM-type spherical motor [5]. Wang *et al.* reported a multi-DOF spherical magnet motor [6]. Furthermore, there are studies on multi-DOF actuators using ultrasonic motors. Bansevicius reported a piezoelectric multi-DOF actuator [7]. Amano *et al.* developed an ultrasonic actuator with multi-DOF [8]. Aoyagi *et al.* constructed a multi-DOF ultrasonic motor using multi-mode ring-form vibrator [9]. Shimoda *et al.* reported an ultrasonic motor for driving spherical surface [10]. The actuators can provide multi-DOF motion using single stators, however, they cannot be used in place of multi-DOF motion units using several electromagnetic motors because of their complex structures, small output torque, difficulties in control, and so on.

According to the state of multi-DOF actuators as mentioned above, the authors have developed a multi-DOF ultrasonic motor [11][12]. The multi-DOF ultrasonic motor provides three-DOF rotation of a spherical rotor using three orthogonal natural vibration modes of a Langevin type stator. In order to put the multi-DOF ultrasonic motor into practice, a novel controller for the motor is constructed in this study. First, an inverse model of the multi-DOF ultrasonic motor is constructed using experienced knowledge about ultrasonic motors by designers and neural network technique in order to deal with the redundancy and non-linear characteristics of the motor. A neural network based inverse model of a single-DOF ultrasonic motor has been reported by Lin *et al.* [13]. In their model, however, only single operating parameter is considered. To fully express the motion of the multi-DOF ultrasonic motor, all potential operating parameters, adds up to six, must be considered. Second, a novel control method for multi-DOF ultrasonic motor using the constructed inverse model is proposed. To confirm their effectiveness, motion control test of the rotor using the inverse model and the control method are conducted.

In this paper, the inverse model is introduced in section 2 for constructing the control method described

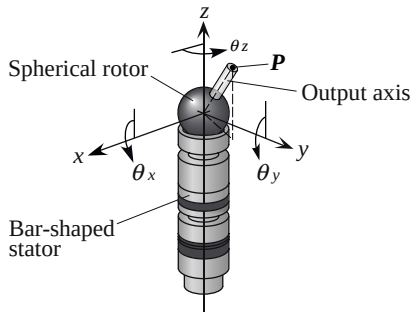

Figure 1: *Multi-DOF ultrasonic motor and its reference frame*

in section 3. Then in section 4, the motion control tests are presented. Finally, conclusions of this study are described in section 5.

2 Inverse Model

The multi-DOF ultrasonic motor consists of a bar-shaped stator and a spherical rotor as shown in Fig. 1. The rotor rotates around the x-, y- and z-axis using a first longitudinal vibration mode and two orthogonal second bending vibration modes of the stator [12]. By combining the rotations around three axes, the rotor is rotated around arbitrary axis. However, the potential operating parameters of the motor are redundant with respect to an arbitrary rotational axis of the rotor. Furthermore, each parameter has non-linear characteristics against the rotational speed [11]. Namely, an inverse model of the multi-DOF ultrasonic motor should be developed to realize the desired rotational axis. So, the inverse model is proposed using our prior knowledge of ultrasonic motors and neural network technique in this section.

2.1 Driving state representation

A representation method of driving state of the rotor is considered.

First, a rotational speed $\boldsymbol{N}$ is defined to express the driving state. The direction and the magnitude of $\boldsymbol{N}$ represent the rotational axis and the rotational speed of the rotor, respectively. Each component represents the rotational speed around each axis of the reference frame in Fig. 1.

Second, considering the driving principle of the multi-DOF ultrasonic motor [12], a relative rotational speed $\boldsymbol{N^r}$ is defined as follows. The driving characteristics around the x- (y-) axis and z-axis are different depending on the driving principle [12], so

Table 1: *Classification of driving state*

	(i) Category			(ii) Sub-category							
class	cat.	$\boldsymbol{N^r}$	Phase relation ●: *Ben_x* ●: *Ben_y* ○: *Lon_z*	sub-cat.	Maximum ingredient	Phase [rad] ϕ_{Ben_x}	ϕ_{Ben_y}	ϕ_{Lon_z}	Relative amplitude A^r_x	A^r_y	A^r_z
1				i	$\lvert N^r_x\rvert$	-π/2~0	π/2	0	A^r_x	1	1
2	I	(+, +, -)	●○● ◄π►	ii	$\lvert N^r_y\rvert$	0	π/2~π	π/2	1	A^r_y	1
3				iii	$\lvert N^r_z\rvert$	0	π/2	0~π/2	1	1	A^r_z
4				i	$\lvert N^r_x\rvert$	π/2~π	π/2	0	A^r_x	1	1
5	II	(+, -, +)	○●○ ◄π►	ii	$\lvert N^r_y\rvert$	π/2	0~π/2	0	1	A^r_y	1
6				iii	$\lvert N^r_z\rvert$	π/2	0	-π/2~0	1	1	A^r_z
7				i	$\lvert N^r_x\rvert$	0~π/2	π/2	0	A^r_x	1	1
8	III	(+, -, -)	○●● ◄π►	ii	$\lvert N^r_y\rvert$	π/2	π/2~π	0	1	A^r_y	1
9				iii	$\lvert N^r_z\rvert$	0	π/2	-π/2~0	1	1	A^r_z
10				i	$\lvert N^r_x\rvert$	0~π/2	0	π/2	A^r_x	1	1
11	IV	(-, +, +)	●○○ ◄π►	ii	$\lvert N^r_y\rvert$	0	-π/2~0	π/2	1	A^r_y	1
12				iii	$\lvert N^r_z\rvert$	π/2	0	π/2~π	1	1	A^r_z
13				i	$\lvert N^r_x\rvert$	-π/2~0	0	π/2	A^r_x	1	1
14	V	(-, +, -)	●●○ ◄π►	ii	$\lvert N^r_y\rvert$	0	0~π/2	π/2	1	A^r_y	1
15				iii	$\lvert N^r_z\rvert$	0	π/2	π/2~π	1	1	A^r_z
16				i	$\lvert N^r_x\rvert$	π/2~π	0	π/2	A^r_x	1	1
17	VI	(-, -, +)	●○○ ◄π►	ii	$\lvert N^r_y\rvert$	π/2	-π/2~0	0	1	A^r_y	1
18				iii	$\lvert N^r_z\rvert$	π/2	0	0~π/2	1	1	A^r_z
19				i	$\lvert N^r_x\rvert$	-π~-π/2	π/2	0	A^r_x	1	1
20	VII	(+, +, +)	●●○ ●●○ ○●● ◄2π►	ii	$\lvert N^r_y\rvert$	0	-π~-π/2	π/2	1	A^r_y	1
21				iii	$\lvert N^r_z\rvert$	π/2	0	-π~-π/2	1	1	A^r_z
22				i	$\lvert N^r_x\rvert$	π/2~π	-π/2	0	A^r_x	1	1
23	VIII	(-, -, -)	●○● ○●● ●●○ ◄2π►	ii	$\lvert N^r_y\rvert$	0	π/2~π	-π/2	1	A^r_y	1
24				iii	$\lvert N^r_z\rvert$	-π/2	0	π/2~π	1	1	A^r_z
25		$(N^r_x, 0, 0)$				0	0, π/2	π/2, 0	0	1	1
26		$(0, N^r_y, 0)$				0, π/2	0	π/2, 0	1	0	1
27		$(0, 0, N^r_z)$				0, π/2	π/2, 0	0	1	1	0
28		$(N^r_x, N^r_y, 0)$				0, π/2, 0, π/2	π, π/2, 0, 3π/2	π/2, 0, π/2, 0	A^r_x	A^r_y	1

we should scale $\boldsymbol{N}$ to the difference as,

$$N^r_\xi = \begin{cases} N_\xi / N^{xy}_{sta} & (\xi : x, y) \\ N_\xi / N^{z}_{sta} & (\xi : z) \end{cases} \tag{1}$$

where, N^r_ξ is the ξ-component of a scaled rotationl speed. ξ represents coordinates. N^{xy}_{sta} and N^z_{sta} are standard rotational speeds around the x- (y-) axis and the z-axis, respectively, which are obtained using the forward model of the multi-DOF ultrasonic motor developed in our previous study [11].

2.2 Classification of driving state

The diving state is expressed by $\boldsymbol{N^r}$ as mentioned above. The signs of each component of $\boldsymbol{N^r}$ represent the rotational directions. The rotational directions around the x-, y- and z-axis are related to phase differences of two combined vibrations, which are respectively used to generate the rotations around the x-, y- and z-axis. So, the driving state is classified into eight categories considering the signs of each component of $\boldsymbol{N^r}$. The categories represent quadrant where $\boldsymbol{N^r}$ exists. Then, the phase relation between three vibrations is determined as Table 1 (i), while there still remains a certain range for each phase.

Our experiences in ultrasonic motors suggest the exact value of each phase. That is, the phase difference between the combined vibrations for the rota-

tion around each axis should be quarter cycle in order to improve the efficiency of the rotation. According to the knowledge, we determine that the phase difference between two vibrations related to maximum component of $\boldsymbol{N^r}$ is made to be quarter cycle, and that the relative amplitude of the vibrations are to be 1.0. So, the driving state is still classified into three sub-categories considering the absolute value of components of $\boldsymbol{N^r}$. Then, the phases and relative amplitudes for two of three vibrations are exactly determined as in Table 1 (ii).

Still more, we must consider some special cases of driving states. The cases are when the rotational axis agrees with the x-, y- or z-axis, and when it exists in the xy plane. In the former case, the two vibrations are only used to generate the rotational axis, and the phase difference between them is to be $\pi/2$. In the latter case, the phase difference between the two bending vibrations is to be 0 or π, and that between bending and longitudinal vibrations is to be $\pi/2$. These cases are particularly classified from class 25 to class 28 as shown in Table 1.

According to the classification mentioned above, the driving state of rotor is divided into 28 states. By the classification, the problems for the redundancy of operating parameters against the driving state is solved.

2.3 Non-linear mapping

Two operating parameters, the phase and relative amplitude of one vibration, for class 1 to class 24 in Table 1 are still remained to be determined. Their exact values cannot be easily determined because they have non-linear characteristics against the driving state. For example, the characteristic between $\boldsymbol{N^r}$ and phase and that between $\boldsymbol{N^r}$ and amplitude of class 1 are shown in Fig. 2. The characteristics are obtained by the forward model [11], where relative amplitude of x-component of $\boldsymbol{N^r}$ is 1.0. According to the non-linearity, the neural network technique is used to map the characteristics.

A three-layer neural network with two and one units respectively in sensory and response layers is used for mapping the characteristics of each parameter. Sigmoid function is adopted in the units for the sensory and associate layers, and linear function is for the response layer. The sensory and associate layers have another unit for threshold.

For training the neural networks for each class, teacher signals are obtained using the forward model [11]. Connective weights of the neural networks are trained using the error back propagation method [13]. The relationships between the teacher signals and outputs from neural network in case of class 1 are shown in Fig. 3, where the training conditions

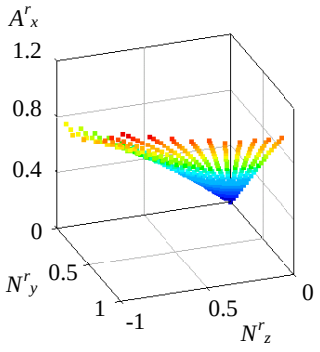

(a) Relative amplitude

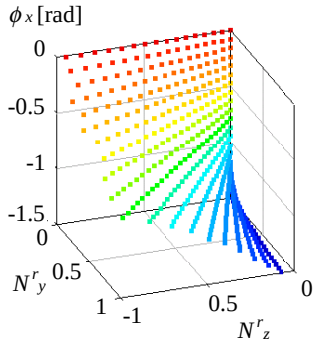

(b) Phase

Figure 2: *Non-linear characteristics of operating parameter*

are as follows: numbers of teacher signals, training cycle and units in associate layer are 1000, 30000 and 5, respectively. Initial connective weights are set to be random value between -3 and 3. A training rate is 0.5. The non-linear characteristics shown in Fig. 2 are well mapped after the training. The errors between the teacher signals and outputs are within 0.5 % of full scale. The neural networks for other classes are successfully trained as well.

2.4 Construction of inverse model

The inverse model of the multi-DOF ultrasonic motor is constructed using the above-mentioned classification and neural network. The block diagram of the inverse model is shown in Fig. 4. A classifier divides the desired rotational axis into 28 classes in Table 1. Then, according to the class, a linear transducer for class 25 to class 28 or a neural network transducer for class 1 to class 24 is alternatively used to provide the phases and relative amplitude of three natural vibrations.

2.5 Numerical simulation on inverse model

In order to confirm the effectiveness of the inverse model, the step responce of a location of the output

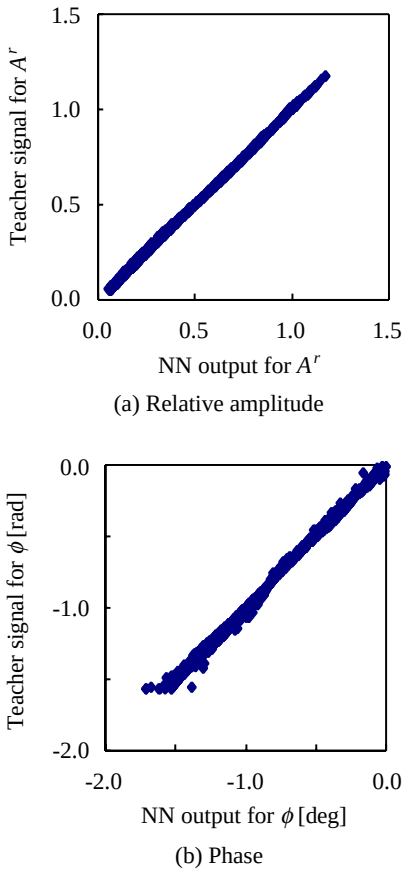

Figure 3: *Result of neural network training*

axis $\boldsymbol{P}$ shown in Fig. 1 is conducted using the inverse model in numerical simulation. For comparison, the location of the output axis $\boldsymbol{P}$ is also controlled combining the rotation around the x- and y-axis in series. The starting and destination locations of $\boldsymbol{P}$ are (1.00, 0.00, 0.00) and (0.29, -0.83, 0.48), respectively. The history plot of $\boldsymbol{P}$ is shown in Fig. 5. It can be seen that the location of $\boldsymbol{P}$ moves on the shortest path between the staring/destination locations only when the inverse model is used.

3 Control Method

The control method for the multi-DOF ultrasonic motor is proposed using the inverse model in this section. The block diagram of the control method is shown in Fig. 6, where the control parameter $\boldsymbol{P}$ and the desired parameter $\boldsymbol{P_d}$ are the present and desired locations of the output axis in Fig. 1, respectively. Each block plays the following roles.

Rotational Axis Identifier: A rotational axis identifier provides the desired rotational axis $\boldsymbol{N^d}$ using the

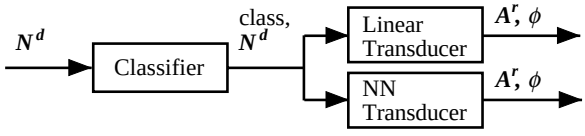

Figure 4: *Block diagram of inverse model*

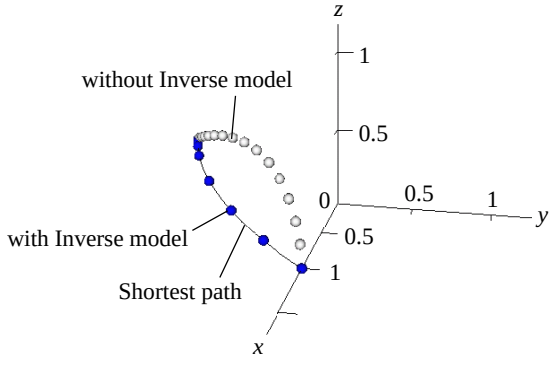

Figure 5: *Simulated result of step responce*

following equation.

$$\boldsymbol{N^d} = \frac{\boldsymbol{P} \times \boldsymbol{P_d}}{|\boldsymbol{P} \times \boldsymbol{P_d}|} \tag{2}$$

Inverse Model: The inverse model determines the phases $\boldsymbol{\phi}$ and relative amplitudes $\boldsymbol{A^r}$ of three alternating inputs for the multi-DOF ultrasonic motor (*cf.* section 2).

Multiple Rate Identifier: A multiple rate identifier provides the multiple rate C_A of amplitudes for three alternating inputs. For example, it is constructed using the proportional control as follows.

$$\begin{cases} C_A = K_p \cdot \Delta\theta \\ \Delta\theta = \cos^{-1} \dfrac{|\boldsymbol{P} \cdot \boldsymbol{P_d}|}{|\boldsymbol{P}||\boldsymbol{P_d}|} \end{cases} \tag{3}$$

where K_p is the proportional feedback again, and $\Delta\theta$ is the angle between $\boldsymbol{P}$ and $\boldsymbol{P_d}$.

Amplitude Calculator: An amplitude calculator determines the amplitudes $\boldsymbol{A}$ of three alternating inputs from the relative amplitudes $\boldsymbol{A^r}$ and the multiple rate C_A using the following equation.

$$\boldsymbol{A} = C_A \cdot \boldsymbol{A^r} \tag{4}$$

Driving Circuit: The phases and amplitudes of three inputs are determined using the blocks as mentioned

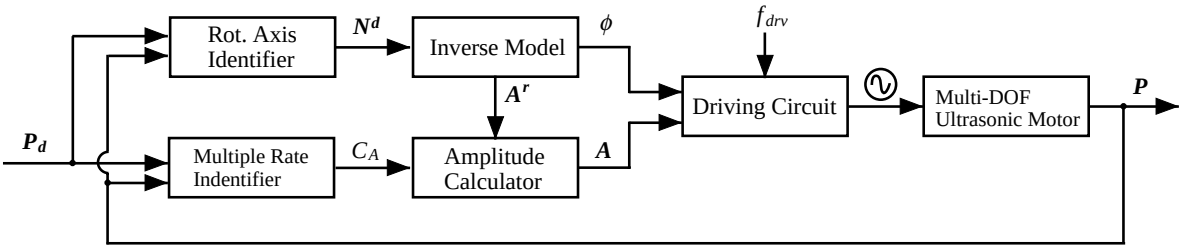

Figure 6: *Block diagram of control method*

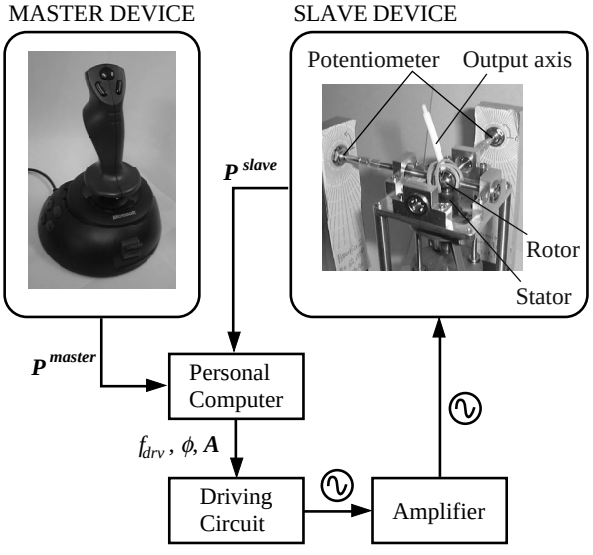

Figure 7: *Experimntal system*

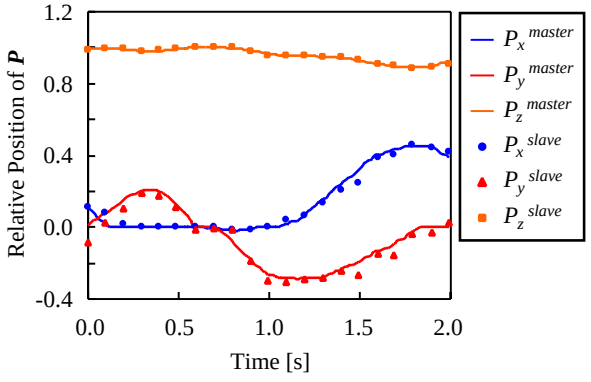

(a) History plot of the location of output axis

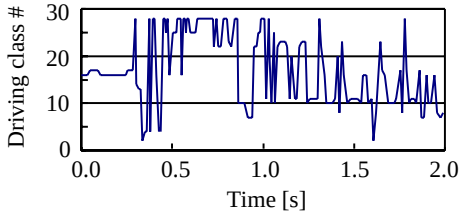

(b) History of driving class

Figure 8: *Experimntal result for motion control test*

above. The driving circuit provides three alternating voltages according to the decided parameters, while the driving frequencies f_{drv} of the inputs are set to be equal to the corresponded natural frequencies f_0 of three vibrations used in the multi-DOF ultrasonic motor.

4 Experiment

An experiment for controlling the location of the output axis $\boldsymbol{P}$ is performed using the proposed control method. The experimental system is shown in Fig. 7. The system is constructed as a mster-slave system. The joystick (Microsoft SideWinder) is used as a master device to present the desired location of the output axis $\boldsymbol{P_d}$. The location of the output axis $\boldsymbol{P}$ is measured using potentiometers as shown in Fig. 7. The controller is implemented on a personal computer. An experimental result is shown in Fig. 8, where the driving frequency f_{drv} and maximum input voltage are 39.8 kHz and 24 V, respectively. Fig. 8 (a) shows the history plot of $\boldsymbol{P}$, and Fig. 8 (b) shows the history of the driving class (cf. Table 1). It is seen from Fig. 8 (a) that the location $\boldsymbol{P}$ of the slave device successfully follows that of the master device using the inverse model based controller. During the control, it is also seen from Fig. 8 (b) that the driving class is successfully switched in the inverse model.

The control method using the proposed inverse model can be used not only for our motor but also for the other multi-DOF ultrasonic motors [7][8][9].

5 Conclusions

The control method of the multi-DOF ultrasonic motor is developed in the present study. First, the inverse model of the multi-DOF ultrasonic motor is constructed. The inverse model successfully provides the input parameters for the ultrasonic motor with respect to the desired rotational axis of the rotor. In other word, the inverse model makes the spherical rotor be able to rotate around an arbitrary rotational axis. It is clarified from the process of constructing the inverse model that the problems of the redundant and non-linear characteristics of the multi-DOF ultrasonic motor are solved using our prior knowledge of ultrasonic motors and neural network technique. Second, the control method is proposed using the inverse model. The location of output axis of the rotor can be controlled to the desired point using the control method. Finally, effectiveness of the proposed control method is confirmed by the experiment.

Future study focuses on applying the multi-DOF ultrasonic motor to an active endoscope and multi-DOF robots.

Acknowledgments

This research is supported in-part by Canon Inc.

References

[1] R.B. Roth and Kok-Meng Lee: "Design Opimization of a Three Degrees-of-Freedom Variable-Reluctance Spherical Wrist Motor,"Trans. ASME J. Engineering for Industry, Vol. 117, pp. 378-388, 1995.

[2] T. Yano, T. Suzuki, M. Sonoda and M. Kaneko: "Basic Characteristics of the Developed Spherical Stepping Motor,"Proc. 1999 IEEE/RSJ Int. Conf. Intelligent Robots and Systems, Vol. 3, pp. 1393-1398, 1999.

[3] T. Yano, M. Kaneko and M. Sonoda: "Development of a Synchronous Motor With Three Degrees of Freedom,"Proc. Theory and Practice of Robots and Manipulators 10:The 10th CISM-IFToMM Symposium, Vol. 2, 1997.

[4] S. M. Sokolov, O. V. Trifonov and V. S. Yaroshevsky: "Research of Spherical Derect Drive Actuators Control System,"Proc. 2001 IEEE International Conference on Robtics and Automation, pp. 1780-1785, 2001.

[5] D. Ebara, N. Katsuyama and M. Kajioka: "Research of Spherical Derect Drive Actuators Control System,"Proc. 2001 IEEE International Conference on Robtics and Automation, pp. 1792-1797, 2001.

[6] J. Wang, K Mitcell, G. W. Jewell, and D. Howe: "Multi-Degree-of-Freedom Spherical Magnet Motors,"Proc. 2001 IEEE International Conference on Robtics and Automation, pp. 1798-1805, 2001.

[7] Ramutis Bansevicius: "Piezoelectric Multi-Degree-of-Freedom Actuators/Sensors,"Proc. 3rd Int. Conf. Motion and Vibration, pp. K9-K15, 1996.

[8] T. Amano, T. Ishii, K. Nakamutra and S. Ueha: "An Ultrasonic Actuator with Multi-degree of Freedom Using Bending and longitudinal Vibrations of a sSingle Stator,"Proc. IEEE Ultrasonics Symposium, Vol. 1, pp. 667-670, 1998.

[9] M. Aoyagi, Y. Tomokawa and T. Takano: "Construction of Multi-Degree-of-Freedom Ultrasonic Motor using Multi-mode Ring-form Vibrator,"Proc. 1999 Spring Meetng of the Acoustical Society of Japan, Vol. II, pp. 979-980, 1999.

[10] S. Shimoda, M. Ueyama, S. Matsuda, T. Matsuo, K. Sasaki and K. Itao: "Design of Ultrasonic Motor for Driving Spherical Surface,"Proc. Int. Conf. Machine Automation 2000, pp. 255-260, 2000.

[11] K. Takemura, D. Harada and T. Maeno: "A Master-Slave System using a Multi-DOF Ultrasonic Motor and its Controller designed considering Measured and Simulated Driving Characteristics,"Proc. 2001 IEEE/RSJ Int. Conf. Intelligent Robots and Systems, pp. 1977-1982, 2001.

[12] K. Takemura and T. Maeno: "Design and Control of an Ultrasonic Motor Capable of Generating Multi-DOF Motion,"IEEE/ASME Trans. Mechatronics, Vol. 6, No. 4, pp. 499-506, 2001.

[13] Faa-Jeng Lin, Rong-Jong Wai and Sheng-Long Wang: "A Fuzzy Neural Network Controller for Parallel-Resonant Ultrasonic Motor Drive,"IEEE Trans. Industry Electronics, Vol. 45, No. 6, pp. 928-937, 1998.